INFLUENCE OF ANNEALING CONDITIONS ON STRUCTURE AND CRITICAL PARAMETERS OF $Ni_{50}Mn_{37}Sn_{13}$ MAGNETOCALORIC MATERIAL

NGUYEN HUY DAN
Institute of Materials Science, Vietnam Academy of Science and Technology
18 Hoang Quoc Viet, Cau Giay, Hanoi, Vietnam.

NGUYEN MANH AN
Hong Duc University, 565 Quang Trung St., Thanh Hoa City, Vietnam

E-mail: dannh@ims.vast.ac.vn

Abstract. *In this paper, we present the influence of annealing conditions on structure and magnetic behavior of $Ni_{50}Mn_{37}Sn_{13}$ magnetocaloric alloy prepared by arc-melting technique. The results show that the almost single phase of the full Heusler structure of Ni_2MnSn could be achieved by appropriate annealing. The transformation between martensite and austenite phases, and multi-magnetic phase behavior are observed more clearly with higher fraction of Ni_2MnSn phase. By using Arrott-Noaks method, critical parameters were determined to be $\beta = 0.464 \pm 0.021$, $\gamma = 1.117 \pm 0.073$ and $\delta = 3.41$, which lay between mean-field model ($\beta = 0.5$ and $\gamma = 1$, $\delta = 3$) with long-range ferromagnetic orders and 3D Heisenberg model ($\beta = 0.365$, $\gamma = 1.336$, $\delta = 4.66$) with short-range ferromagnetic orders. The calculated results are in good accordance with the experimentally observed coexistence of weak-ferromagnetic martensite and strong-ferromagnetic austenite phases.*

Keywords: Giant magnetocaloric effect, Heusler alloys, Arrott-Noaks Plot, Magnetic transition.

I. INTRODUCTION

Ni-Mn-Sn Heusler alloys have been attracting a lot of scientists by virtue of their giant magnetocaloric effect (GMCE) and application potential for magnetic refrigeration at room temperature [1-9]. Both the positive (inverse) and negative (normal) GMCEs could be observed in these alloys by changing composition and fabrication conditions. The positive GMCE is believed to relate to a transformation between martensite and austenite phases. The coexistence of ferromagnetic (FM) and antiferromagnetic (AFM) orders was also observed in the alloys. Adding other elements such as Cu, Co, Al...[10-14] and changing fabrication conditions [15-17] are common ways to understand the magnetic mechanism and achieve the desired GMCEs for the alloys. The magnetic orders and the magnetocaloric effects in Ni-Mn-Si alloys were found to be very sensitive to their composition and fabrication conditions.

In this work, we investigated influence of annealing conditions on structure and magnetic behavior of the $Ni_{50}Mn_{37}Sn_{13}$ magnetocaloric alloy prepared by arc-melting technique. Critical parameters of the alloy were determined by using Arrott-Noakes method.

II. EXPERIMENTAL

$Ni_{50}Mn_{37}Sn_{13}$ ingot was prepared by arc-melting method from pure elements ($> 3N$) and then annealed at different annealing temperatures ($T_a = 700 - 1100$°C) for various time ($t_a = 2$ – 16 h) in vacuum. Because Mn is evaporated during arc-melting, an excess of 15 *wt%* of Mn was added to the nominal composition. This compensation amount of Mn was determined basing on thoroughly investigations of the loss of 3 *wt%* of Mn after each time of arc-melting in the same preparation conditions and each sample was arc-melted five times. The structure of the samples were analyzed by X-ray diffraction (XRD) using a Siemens D5000 X-Ray diffractometer with CuK_{α} radiation (λ = 1.54056 Å). The magnetization measurements were performed on Vibrating Sample Magnetometer (VSM). Critical parameters of the alloy were determined by using Arrott-Noakes method and then compared with standard models.

III. RESULTS AND DISCUSSION

Fig. 1 shows room temperature powder-XRD patterns with 2θ range of 20 - 70 ° of the $Ni_{50}Mn_{37}Sn_{13}$ alloys annealed in various conditions. Crystalline phases of Ni_3Sn_2, Mn_3Sn, Ni_2MnSn, $Ni_{1.77}Sn$, $MnSn_2$, $Mn_{1.77}Sn$ and Mn_3Sn_2 are identified from these patterns. The number and relative intensity of diffraction peaks, i.e. crystalline structure, are varied with varying the annealing conditions. It should be noted that the Ni_2MnSn phase is dominated with T_a = 900 - 1000°C and t_a = 2 - 4 h. Especially, the alloy is almost single phase of Ni_2MnSn with T_a = 1000°C and t_a = 2 h.

The effect of the annealing process on the magnetic behavior of the alloy is clearly observed by the thermomagnetization measurements, M(T). Fig. 2 presents thermomagnetization curves in an applied field of 100 Oe for the annealed alloys. The multi-magnetic phase behavior is observed on these M(T) curves. The first phase has Curie temperature (T_C) around 250 K and the second one has T_C in range from 300 K to 350 K. This behavior can be explained by the structural transformation at certain temperatures leading to the transition of the magnetic phases in the annealed alloys. It is supposed that both the martensite and austenite phases can exist in the Ni-Mn-Sn alloys with appropriate Sn-concentration and annealing conditions. The austenite phase is strong-ferromagnetic, while the martensite phase relates to weak-ferromagnetic or anti-ferromagnetic phases [10-12]. In general, by heating up the multi-phase Ni-Mn-Sn alloys from low temperature, the magnetization decreases to a minimum at the temperature T_C^A (Curie temperature of martensite) or T_f^M (martensite finishes) then start to increases fast at the temperature T_s^A (austenite starts). The fast increase stops at the temperature T_f^A (austenite finishes). The last magnetic transition of the ferromagnetic to paramagnetic phases occurs at the temperature T_C^A (Curie temperature of austenite). It should be noted that, the volume fraction of the martensite strongly depends on the fabrication conditions. The martensite phase greatly influences on the positive magnetocaloric effect of the Ni-Mn-Sn alloys [1-7].

In order to complete understanding the second order phase transition (SOPT) and magnetic entropy change, M(H) curves (Fig. 3a) in the vicinity of Curie temperature the $Ni_{50}Mn_{37}Sn_{13}$
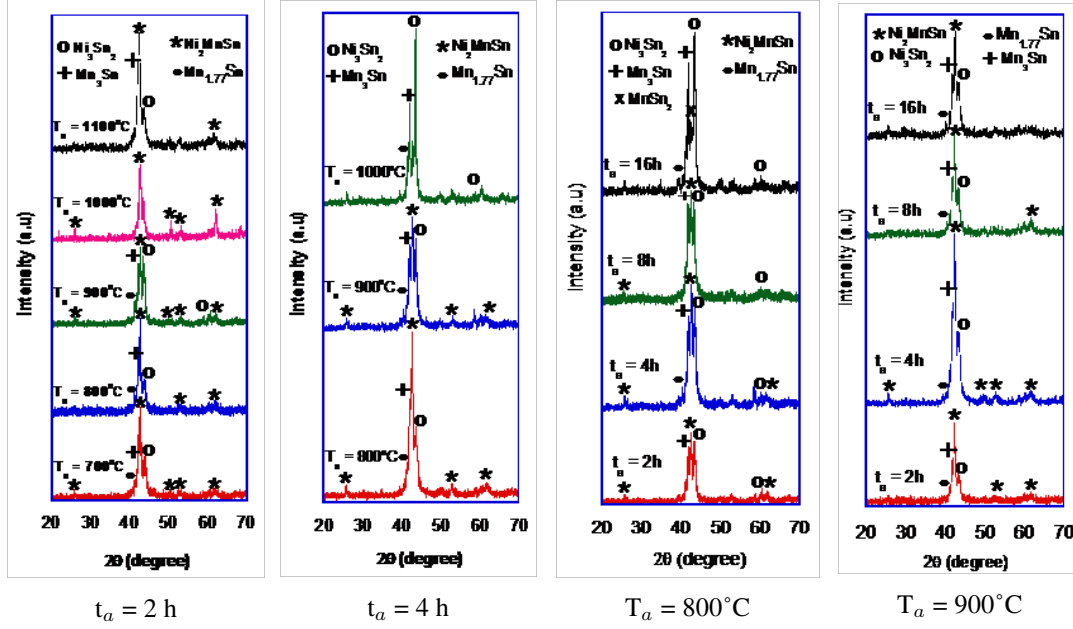
Fig. 1. XRD patterns of the $Ni_{50}Mn_{37}Sn_{13}$ samples annealed in various conditions (T_a - annealing temperature, t_a - annealing time).

sample annealed at 1000°C for 2 hours were performed and analyzed by using Arrott-Noakes method [18, 19]. Because the ferromagnetic-to-paramagnetic transition at Curie temperature is continuous phase transition, the power law dependence of spontaneous magnetization $M_s(T)$ and inverse initial susceptibility $\chi_0^{-1}(T)$ on reduced temperature $\varepsilon = (T - T_C)/T_C$ with the set of critical exponents of β, γ, and δ can be expressed as the following:

$$M_S(T) = M_0(-\varepsilon)^\beta \varepsilon < 0, \tag{1}$$

$$\chi_0^{-1} = (H_0/M_0)\varepsilon^\gamma \varepsilon > 0, \tag{2}$$

At Curie temperature T_C, the exponent δ determined by magnetization and applied magnetic field:

$$H = DM^\delta \varepsilon \quad = \quad 0, \tag{3}$$

where M_0, H_0/M_0 and D are the critical amplitudes.

Arrott plots, M^2 versus H/M, (Fig. 3b) are derived from M(H) curves at various temperatures (Fig. 3a). The spontaneous magnetization $M_s(T)$ and initial inverse susceptibility $\chi_0^{-1}(T)$ of the sample with $T_a = 1000$°C and $t_a = 2$ h are achieved from extrapolating and linearly fitting of Arrott plots M^2 versus H/M at high magnetic field. These values of $M_s(T)$ and $\chi_0^{-1}(T)$ are presented as functions of temperature T (Fig. 4). In accordance with equation (1) and (2) for $M_s(T)$ and $\chi_0^{-1}(T)$, the power law fits are used to extract β, γ and T_C (Fig 4a and 4b).

The fittings of $M_s(T)$ and $\chi_0^{-1}(T)$ data give the values of $\beta = 0.464 \pm 0.021$, $T_C = 309.62 \pm 0.11$ and $\gamma = 1.117 \pm 0.073$, $T_C = 309.51 \pm 0.22$, respectively. The value of δ can be obtained by using equation (3) or the Wildom scaling equation [20]:
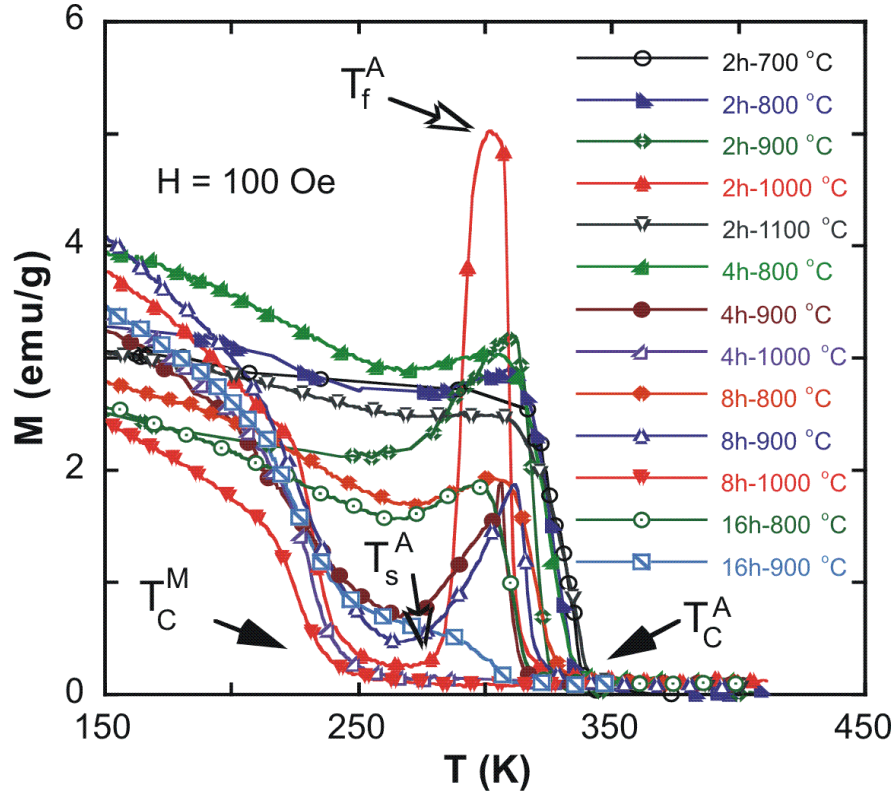
Fig. 2. Themomagnetization curves in an applied field of 100 Oe of the $Ni_{50}Mn_{37}Sn_{13}$ samples annealed in various conditions.

$$\delta = 1 + \gamma/\beta \qquad (4)$$

From the values of β and γ of our above obtained results, the calculated values of δ are 3.41.

In comparison with some standard models [21] including mean-field model ($\beta = 0.5$, $\gamma = 1$, $\delta = 3$), 3D Heisenberg model ($\beta = 0.365$, $\gamma = 1.336$, $\delta = 4.66$) and 3D Ising model ($\beta = 0.325$, $\gamma = 1.241$, $\delta = 4.82$), we can realize that our results are closer to mean-field model. This means, the sample is mainly of long-range ferromagnetic order. However, all the critical parameters of the sample fall between those of mean-field model and 3D Heisenberg model revealing a part of short-range order coexists with long-range order of ferromagnetic interactions in the material. The coexistence of the short- and long-range orders is in good agreement with the above-mentioned multi-magnetic phase behavior and martensite-austenite transformation.

The critical parameter $\beta = 0.501$ obtained for the $Ni_{50}Mn_{30}Sn_{20}$ bulk sample is very close to that of mean-field model (long-range ferromagnetic order) in accordance with single austenite phase and singe phase magnetic behavior [8]. As for the $Ni_{50}Mn_{37}Sn_{13}$ ribbon sample, with $\beta = 0.385$ close to 3D Heisenberg model (short-range ferromagnetic order), the coexistence of the martensite and austenite phases as well as the coexistence of short-range antiferromagnetic and
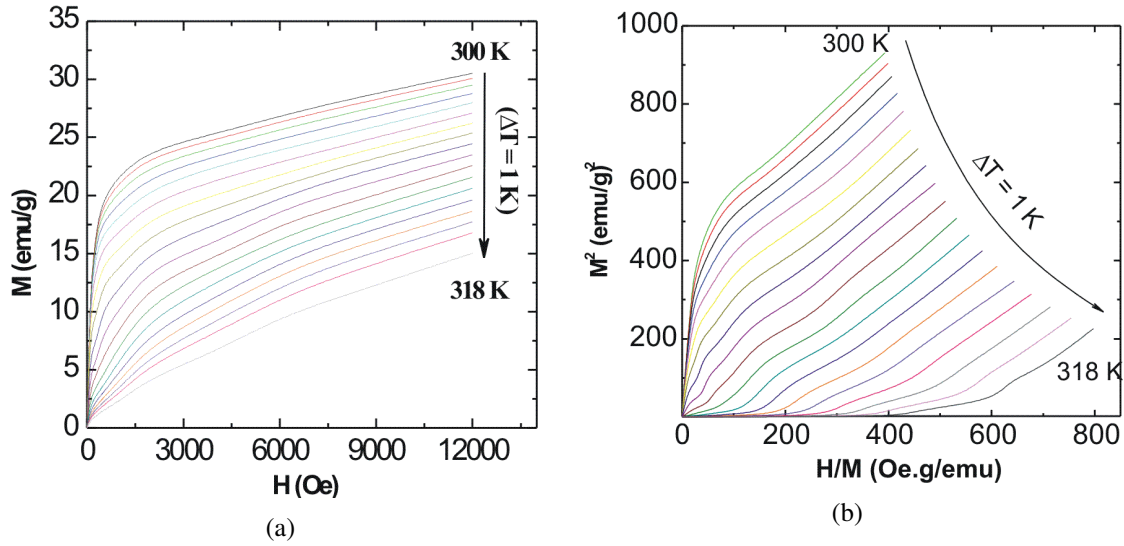
Fig. 3. Field dependences of magnetization (a) and Arrott plots (b) of the $Ni_{50}Mn_{37}Sn_{13}$ sample annealed at 1000°C for 2 hours.

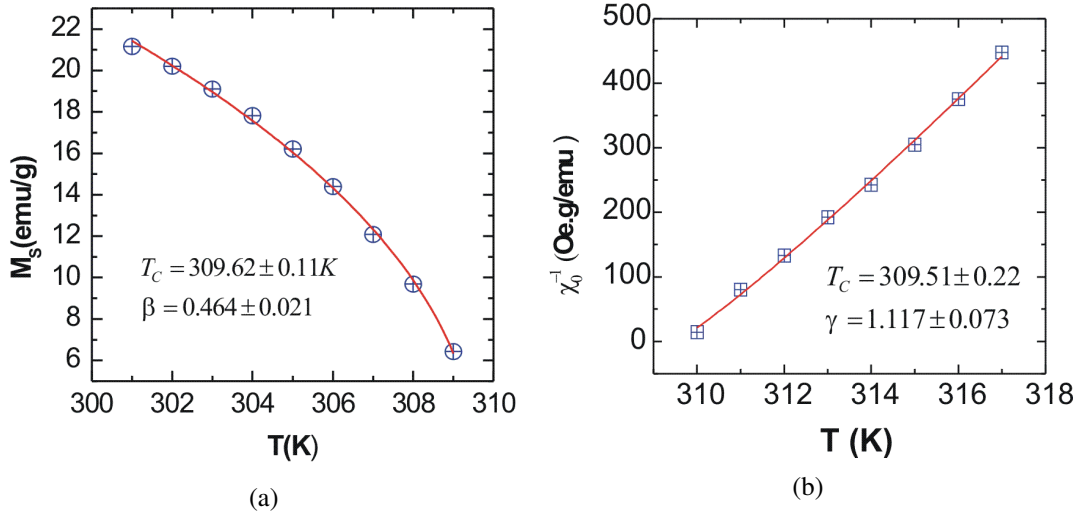**Fig. 4.** Temperature dependences of spontaneous magnetization M_s (a) and the inverse initial susceptibility χ_0^{-1} (b) of the $Ni_{50}Mn_{37}Sn_{13}$ sample annealed at 1000°C for 2 hours.

long-range ferromagnetic phases was clearly observed [9]. Thus, magnetic orders in Ni-Mn-Sn alloys are very sensitive to composition and fabrication conditions.

IV. CONCLUSION

The influence of annealing conditions on structure and magnetic behavior of $Ni_{50}Mn_{37}Sn_{13}$ magnetocaloric alloy has been investigated. The almost single phase of the full Heusler structure of Ni_2MnSn could be achieved by appropriate annealing. The critical parameters obtained by using Arrott-Noakes method are useful for predicting structural and magnetic behaviors of the material. The coexistence of long-range ferromagnetic (FM) and short-range ferromagnetic or antiferromagnetic (AFM) orders in Ni-Mn-Sn could be controlled by fabrication conditions.

REFERENCES

[1] T. Krenke, E. Duman, M. Acet, E. F. Wassermann, X. Moya, L. Mañosa, and A. Planes, *Nature Mater.* **4** (2005) 450.

[2] T. Krenke, M. Acet, E. F. Wassermann, X. Moya, L. Mañosa, and A. Planes, *Phys. Rev. B* **72** (2005) 014412.

[3] P. J. Shamberger, and F. S. Ohuchi, *Phys. Rev. B* **79** (2009) 144407.

[4] V. V. Khovaylo, K. P. Skokov, O. Gutfleisch, H. Miki, T. Takagi, T. Kanomata, V. V. Koledov, V. G. Shavrov, G. Wang, E. Palacios, J. Bartolomé, and R. Burriel, *Phys. Rev. B* **81** (2010) 214406.

[5] D. L. Schlagel, W. M. Yuhasz, K. W. Dennis, R. W. McCallum, and T. A. Lograsso, *Scripta Mater.* **59** (2008) 1083.

[6] Y. B. Yang, X. B. Ma, X. G. Chen, J. Z. Wei, R. Wu, J. Z. Han, H. L. Du, C. S. Wang, S. Q. Liu, Y. C. Yang, Y. Zhang, and J. B. Yang, *J. Appl. Phys.* **111** (2012) 07A916.

[7] E. C. Passamani, V. P. Nascimento, C. Larica, A. Y. Takeuchi, A. L. Alves, J. R. Provetib, M. C. Pereirac, and J. D. Fabrisd, *J. Alloys Comp.* **509** (2011) 7826.

[8] T. L. Phan, N.H. Duc, N.H. Yen, P.T. Thanh, N.H. Dan, P. Zhang P, S.C. Yu, *IEEE Trans. Magn.* **48(4)** (2012) 1381.

[9] T. L. Phan, P. Zhang, N.H. Dan, N.H. Yen, P.T. Thanh, T.D. Thanh, M.H. Phan, and S. C. Yu, *Appl. Phys. Lett.* **101** (2012) 212403.

[10] R. Y. Umetsu, A. Sheikh, W. Ito, B. Ouladdiaf, K.R. A. Ziebeck, T. Kanomata, and R. Kainuma, *Appl. Phys. Lett.* **98** (2011) 042507.

[11] R. Y. Umetsu, A. Fujita, W. Ito, T. Kanomata, and R. Kainuma, *J. Phys. Condens. Matter* **23** (2011) 326001.

[12] Z. Zhong, S. Ma, D. Wang, and Y. Du, *J. Mater. Sci. Technol.* **28** (2012) 193.
B. M. Wang, L. Wang, Y. Liu, and B. C. Zhao, *J. Appl. Phys.* **105** (2009) 023913.

[13] V. Basso, C. P. Sasso, K. P. Skokov, O. Gutfleisch, V. V. Khovaylo, *Phys. Rev. B* **85** (2012) 014430.

[14] D. L. Schlagel, R. W. McCallum, T. A. Lograsso, *J. Alloy Compd.* **463** (2008) 38.

[15] I. Babita, S. I. Patil, and S. Ram, *J. Phys. D: Appl. Phys.* **43** (2010) 205002.

[16] S. E. Muthu, N. V. R. Rao, M. M. Raja, S. Arumugam, K. Matsubayasi, and Y. Uwatoko, *J. Appl. Phys.* **110** (2011) 083902.

[17] A. Arrott and J. E. Noakes, *Phys. Rev. Lett.* **19** (1967) 786-789.

[18] S. Rößler, U.K Rößler, K. Nenkov, D. Eckert, S. M. Yusuf, K. Dörr, and K.H. Müller, *Phys. Rev. B* **70** (2004) 104417.

[19] B. Widom, *J. Chem. Phys.* **41** (1964) 1633.

[20] H. E. Stanley, *Oxford University Press*, (1971).